Bioconjugate Chemistry

Communication

"Polymultivalent" polymer/peptide-cluster conjugates for an enhanced targeting of cells expressing ##-integrins

Damien Duret, Adrien Grassin, Maxime Henry, Thibault Jacquet, Fabien Thoreau, Sandrine Denis-Quanquin, Jean-Luc Coll, Didier Boturyn, Arnaud Favier, and Marie-Thérèse Charreyre

Bioconjugate Chem., **Just Accepted Manuscript** • DOI: 10.1021/acs.bioconjchem.7b00362 • Publication Date (Web): 02 Aug 2017

ACS Publications

Bioconjugate Chemistry is published by the American Chemical Society. 1155 Sixteenth Street N.W., Washington, DC 20036

"Polymultivalent" polymer/peptide-cluster conjugates for an enhanced targeting of cells expressing $\alpha_v\beta_3$-integrins

Damien Duret,[a,b] Adrien Grassin,[c] Maxime Henry,[d] Thibault Jacquet,[d] Fabien Thoreau,[c,d] Sandrine Denis-Quanquin,[e] Jean-Luc Coll,[d]* Didier Boturyn,[c]* Arnaud Favier,[a,b]* Marie-Thérèse Charreyre[a,b]

[a] Univ Lyon, Université Lyon 1, INSA de Lyon, CNRS, Laboratoire Ingénierie des Matériaux Polymères, UMR5223, F-69621 Villeurbanne, France.

[b] Univ Lyon, Ens de Lyon, CNRS, Laboratoire Joliot-Curie, USR3010, F-69364 Lyon, France.

[c] Univ. Grenoble Alpes, CNRS, DCM UMR 5250, F-38000 Grenoble, France.

[d] Centre de Recherche UGA-INSERM U1209 - UMR CNRS 5309, Institute for Advanced Biosciences, F-38700 Grenoble, France.

[e] Univ Lyon, Ens de Lyon, CNRS, Université Lyon 1, Laboratoire de Chimie, UMR5182, F-69342 Lyon, France.

Supporting Information Placeholder

ABSTRACT: A new class of "polymultivalent" ligands combining several ligand-clusters and a water-soluble biocompatible polymer is introduced. These original conjugates bear two levels of multivalency. They are prepared by covalent coupling of a controlled number of tetrameric cRGD peptide-clusters along a well-defined copolymer synthesized by RAFT polymerization. The presence of multiple copies of peptide-clusters on the same polymer backbone resulted in a much higher relative potency than the free cluster reference. Thanks to the "polymultivalency", up to ~2 orders of magnitude potency enhancement was reached in a competitive cell adhesion assay (nanomolar range IC_{50} values). In addition, confocal microscopy and flow cytometry demonstrated that fluorescent "polymultivalent" conjugates (emitting in the far-red/near-infrared) were able to specifically and selectively label cells expressing $\alpha_v\beta_3$-integrin, the natural receptor of cRGD.

Biospecific molecular recognition plays a pivotal role in many life processes and often relies on the multivalent interactions between ligands and their target receptors.[1] For several years now, the concept of multivalency has been taken over by chemists to design a wide range of multivalent ligands consisting in several monovalent ligands grafted onto a multifunctional scaffold for diagnostic and/or therapeutic applications.[2]

As reported by Kiessling *et al*., multivalent ligands can interact with their target through various mechanisms, including chelating, subsite binding, statistical rebinding, steric stabilization and clustering effects.[3] Considering ligand systems either soluble or dispersible in water, two categories can be distinguished depending on the size of the scaffold. On the one hand, a large number of clusters of ligands have been prepared from different low molecular weight scaffolds (*ca* <5 000 $g.mol^{-1}$) such as saccharides, cyclens, linear and cyclic peptide/peptoids, porphyrins, cyclodextrins and calixarenes. These clusters have demonstrated an enhanced avidity and selectivity for their target in comparison with the corresponding monovalent ligand. Their interaction with the target is governed by characteristics such as valency, rigidity and spatial organization. On the other hand, a large number of conjugates have been prepared by grafting multiple copies of monovalent ligands on larger scaffolds including polymers, dendrimers, organic and inorganic nanoparticles as well as self-assemblies, liposomes and viruses. Structural and physico-chemical properties of these conjugates, such as size, shape and type of scaffold, nature, density and accessibility of the ligands, proved to be key parameters for their efficiency in biological media. Some of these systems have been used to obtain so-called superselective targeting properties.[4]

To further increase biospecificity, it would be relevant to develop bio-inspired conjugates bearing two levels of multivalency, *i.e.* combining a large multifunctional scaffold (first level of multivalency) and multiple clusters of ligands (second level of multivalency).[5] To our knowledge, there have been very few systems described in the literature. They exclusively refer to nanoparticles or micelles, functionalized with carbohydrate ligand-dendrons. Gillies *et al.*[6] compared nanoparticles functionalized with dendritic and non-dendritic displays of mannose. Similarly, Stenzel *et al.*[7] compared polymer micelles presenting at the surface either glycodendrons (8 glucose residues per dendron) or linear glycopolymer blocks (each bearing on average 9 glucose residues). Moreover, Davis et al.[8] introduced glyco-dendri-protein-nanoparticles with a so-called "nested polyvalency" that were able to potently block viral infections. In all those cases, the two-level multivalent glyconanoparticles demonstrated an enhanced avidity for their targets.

In this study, we designed and evaluated a new class of macromolecular conjugates that can be termed "polymultivalent" ligands. They combine a water-soluble, multifunctional and flexible polymer chain and several ligand-clusters, here peptide-clusters exhibiting each four cyclic RGD ligands (-Arg-Gly-Asp-DPhe-Lys-, named cRGD) (Figure 1). As introduced by Ringsdorf,[9] polymer chains represent an important scaffold family enabling the preparation of a wide array of bioactive conjugates.

RGD, and especially cRGD,[10] peptides are particularly attractive since they exhibit a high affinity for integrins actively involved in processes such as cell adhesion, physiological and tumor angiogenesis.[11] These ligands were shown to efficiently bind integrins both *in vitro* and *in vivo* and are now being clinically evaluated.[12a] RGD ligands are widely used for the targeted delivery of several types of drugs/diagnostic agents and the impact of their multivalent presentation has clearly been established.[12b]

Table 1. Characteristics and IC_{50} values of the various polymer/peptide-cluster conjugates (left) and characteristics of the fluorescent conjugates (right)

Conjugate	M_n [a] ($g.mol^{-1}$)	$n_{cluster}$ [b]	IC_{50} [c] (nM cluster) [relative potency][e]	IC_{50} [d] (nM conjugate) [relative potency][e]
Free cluster	4 447	1	190 ±30 [1]	190 ±30 [1]
C0	62 100	0	None [0]	None [0]
C1.5	76 500	1.5	440 ±70 [0.4]	290 ±50 [0.6]
C4.2	77 900	4.2	33 ±5 [5.6]	8 ±1 [23]
C5.9	84 300	5.9	100 ±20 [1.9]	17 ±4 [11]

Fluorescent conjugate	M_n [a] ($g.mol^{-1}$)	n_f [f]	$n_{cluster}$ [b]
Free cluster[g]	5 454	1	1
C0-Cy5.5[h]	63 900	3.1	0
C0-SulfoCy5.5[g]	65 800	3.7	0
C4.2-Cy5.5[h]	79 900	3.6	4.2
C4.8-SulfoCy5.5[g]	83 800	3.7	4.8

[a] M_n: Number-average molecular weight; [b] $n_{cluster}$: average number of peptide-clusters per conjugate determined by ^1H NMR; [c] Values expressed in molar concentration of peptide-cluster; [d] Values expressed in molar concentration of conjugate (= peptide-cluster concentration/$n_{cluster}$); [e] Relative potency is calculated by dividing the IC_{50} value of the free peptide-cluster by the one of the polymer/peptide-cluster conjugate; [f] n_f: Average number of dyes per polymer chain determined by SEC/UV[13]; [g] Labeled with **SulfoCy5.5**; [h] Labeled with **Cy5.5**.

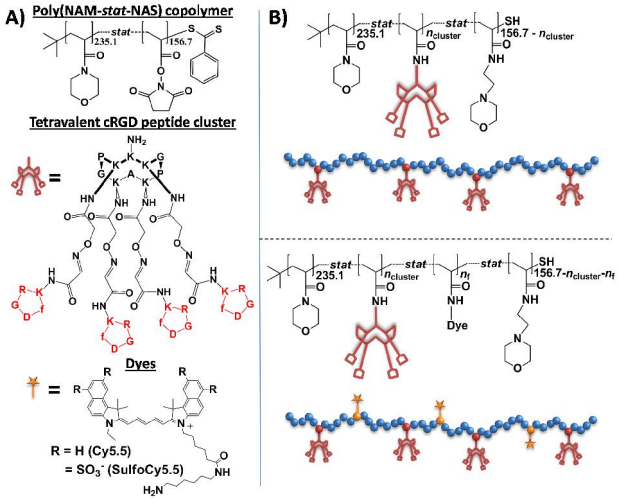

Figure 1. (A) Structure of the reactive copolymer, the tetravalent cRGD peptide-cluster and the cyanine 5.5 dyes (B) Structure and schematic representation of the polymultivalent conjugates.

The tetravalent cRGD-peptide-cluster used in this study (Figure 1A) was prepared from a cyclodecapeptide platform that displays, in a spatially-controlled manner, i) a clustered ligand domain for integrin recognition and, on the opposite side, ii) a lysine primary amine group enabling the regioselective conjugation with different types of entities.[14,15] Thanks to the constrained multivalency, such peptide-cluster has already demonstrated a higher avidity for $\alpha_v\beta_3$-integrins (increased statistical rebinding effects) than the corresponding monovalent cRGD peptide.[14,16] Negative controls with cRAD-peptide-clusters ensured that integrin recognition was specific.[14] In addition, the benefit of the tetrameric cluster compared to the monomeric ligand was confirmed on grafted surfaces.[16c-d] The multivalent effect at 1 nm length-scale (provided by the cluster) could be discriminated from the one at a larger scale (provided by the grafted surface).[16d]

Several cRGD-peptide-clusters were covalently bound along a well-defined reactive copolymer. Poly(*N*-acryloylmorpholine-*stat*-*N*-acryloxysuccinimide), poly(NAM-*stat*-NAS) (Figure 1A), was synthesized by reversible addition-fragmentation chain transfer (RAFT) controlled radical polymerization[17] using a previously optimized procedure.[18] In addition to the inherent advantages of RAFT polymerization, this copolymer exhibits several interesting features. First, NAM units ensure a good water-solubility and biocompatibility. Poly(*N*-acryloylmorpholine) indeed exhibits similar properties to polyethyleneglycol (PEG), known to limit non-specific bio-interactions.[19] Moreover, NAS units provide lateral reactive groups (activated esters) that are regularly-distributed along the polymer backbone at the chosen 60/40 mol% NAM/NAS azeotropic composition.[18a]. Due to the size of the cRGD peptide-cluster (*ca* 4 500 $g.mol^{-1}$), a 60 $kg.mol^{-1}$ copolymer backbone was selected in order to bind several clusters while limiting the effects of steric hindrance on the coupling yield. The conjugation of a controlled number of clusters was achieved by reacting the amine group of the lysine side chain of the peptide-cluster with the activated ester functions of the copolymer, resulting in stable amide bonds. Finally, the remaining activated ester functions were capped with a hydrophilic moiety, aminoethylmorpholine (AEM) (Scheme S1).

In addition to a copolymer bearing no peptide-cluster used as control for the bioassays, three polymer/peptide-cluster conjugates (named polymer/cluster below) were prepared with an increasing average number of clusters per conjugate ($n_{cluster}$ = 1.5, 4.2 and 5.9, respectively) (Table 1, left). Since all the conjugates were highly soluble in aqueous media, they could be thoroughly purified by dialysis.

To quantify the coupling yield, $n_{cluster}$ and to check the efficiency of the purification procedure, the purified conjugates were characterized using both ^1H NMR (500 MHz) and diffusion-ordered NMR spectroscopy (^1H DOSY NMR) (see Supporting Information). ^1H DOSY NMR is indeed able to discriminate peptide-clusters bound along the polymer chain from free peptide-clusters (Figure 2A). The coupling was confirmed as the peptide-cluster and the polymer signals appeared aligned at a same diffusion coefficient ($14 \mu m^2\ s^{-1}$), significantly lower than the one of the free peptide-cluster ($131 \mu m^2\ s^{-1}$, Figure S3). Moreover, no signal corresponding to the free cluster was detected, indicating that the purification procedure was very efficient.

The polymultivalent polymer/cluster conjugates were then evaluated *in vitro* in comparison with the free peptide-cluster reference. The ability of the various conjugates to interact with $\alpha_v\beta_3$-positive cells (HEKβ3) was first investigated in a competitive cell adhesion assay against vitronectin, the natural ligand of $\alpha_v\beta_3$-integrins.[20] The inhibition of HEKβ3 cell adhesion onto vitronectin-coated plates was quantified in the presence of increasing concentrations of conjugates from 0.1 to 10 000 nM (Figure S4, each data point was acquired in triplicates).

These assays provided several important insights (Table 1, left and Figure 2B). As expected, there were no non-specific interactions between the polymer backbone and the integrins. The copolymer **C0** without peptide ($n_{cluster}$ = 0) did not inhibit cell adhesion (Figure S5). Inhibition of cell adhesion was exclusively observed with the polymer/cluster conjugates. For conjugate **C1.5** with $n_{cluster}$=1.5 (IC_{50}=400 nM), the relative potency was lower than for the free cluster (IC_{50}=200 nM) (Table 1, left). This is probably

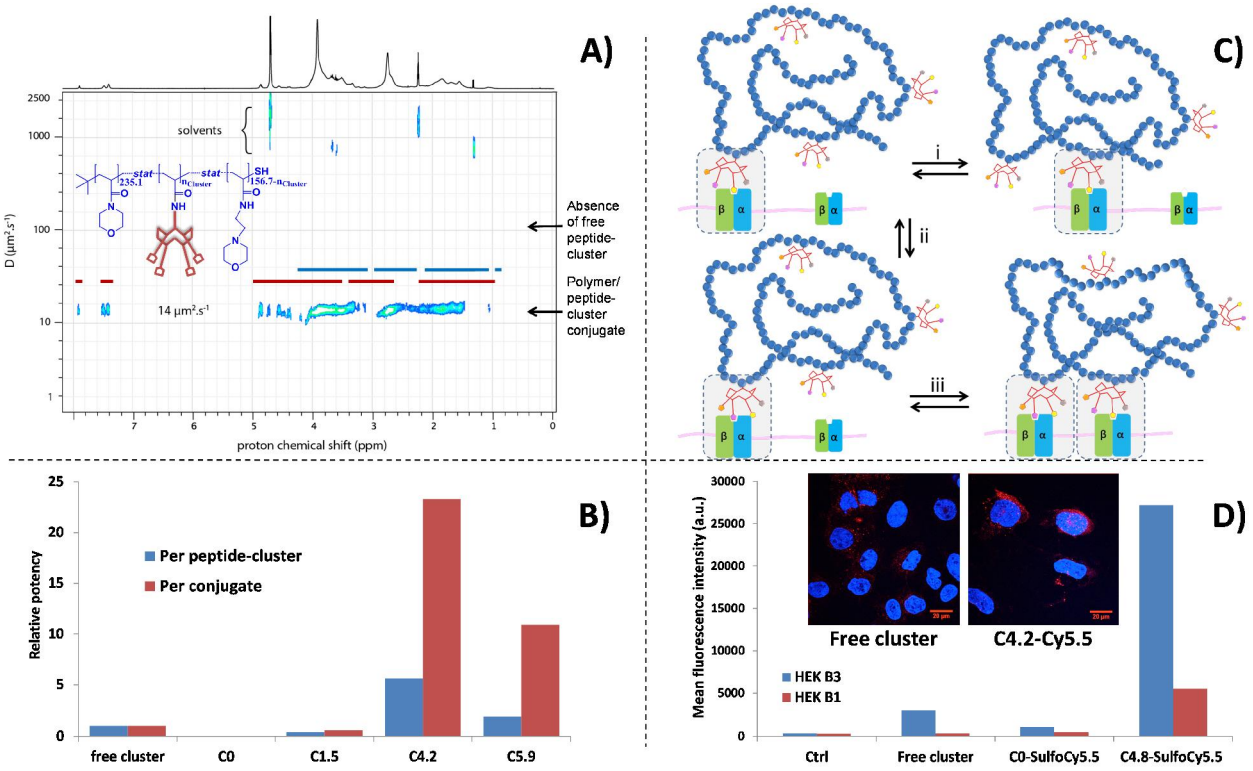

Figure 2. (A) Typical ^{1}H DOSY NMR spectrum of a purified polymer/peptide-cluster conjugate (D_2O/CD_3CN 70/30 v/v, 500 MHz, 298K) showing aligned peptide and polymer signals at a diffusion coefficient D=14µm².s^{-1}. Peptide-cluster peaks (shift range highlighted in red) partially overlap polymer backbone peaks (shift range highlighted in blue). (B) Relative potency (calculated by dividing the IC_{50} value of the free peptide-cluster by the one of the polymer/peptide-cluster conjugate for the various conjugates) expressed either in terms of peptide-cluster concentration, $C_{cluster}$ (blue), or in terms of conjugate concentration, C_{conj} (red), with $C_{cluster} = C_{conj} \times n_{cluster}$., see also Table 1 and Supporting Information (C) Schematic representation of possible interactions between a polymultivalent polymer/peptide-cluster conjugate and a $\alpha_v\beta_3$-integrin presenting target: i and ii illustrate the increased statistical rebinding effect and iii the ability of a polymultivalent conjugate to bind several integrins. Dotted boxes: Zoom on cRGD/integrin interaction (D) Cell labeling quantified by flow cytometry: Mean fluorescence intensity of HEKβ3 (blue histograms) and HEKβ1 (red histograms) cells after incubation with the free cluster, the copolymer without cluster **C0-SulfoCy5.5** and the polymer/peptide-cluster conjugate **C4.8-SulfoCy5.5** at 0.1 µM (peptide-cluster concentration). Ctrl = control with cells only. λ_{exc}=640 nm. Inserts: Confocal microscopy images of HEKβ3 cells labeled with the free cluster (left) and the conjugate **C4.2-Cy5.5** (right) at 0.1 µM (peptide-cluster concentration). Dyes (red, λ_{exc}= 633 nm), nuclei (blue, λ_{exc}= 405 nm). Scale bar = 20 µm. See also Supporting Information

due to steric effects since the polymer chain may limit the accessibility of the lateral peptide-cluster (Scheme S2). However, further increasing $n_{cluster}$ resulted in a significant decrease of the IC_{50} value, thus in a much higher integrin binding efficiency and relative potency. The polymultivalent conjugate **C4.2** with $n_{cluster}$=4.2 offered the best compromise (**C5.9** conjugate with $n_{cluster}$ = 5.9 exhibited a slightly higher IC_{50} value probably due to crowding effects). The inhibition of cell adhesion was effective for **C4.2** concentrations as low as 10 nM. Interestingly, each individual peptide-cluster within the **C4.2** conjugate exhibited a relative potency 6-fold higher than the free peptide-cluster. Considering the relative potency of the conjugate itself, it was 23-fold higher compared to the same reference.

This remarkable result was attributed to several synergetic effects originating from the polymultivalent structure of the polymer/cluster conjugate. Statistical rebinding effects[3] increase with the local concentration of cRGD. Rebinding may occur with cRGD from the polymer chain (Figure 2C, i) and within the peptide-cluster (Figure 2C, ii). Moreover, stabilization of the conjugate-cell interaction is increased by the ability of the conjugate to bind several integrins (Figure 2C, iii). It is important to note that this cooperative (or "zip") effect greatly contributes to the enhanced avidity and may favor integrin clustering at the cell surface. (see also Supporting Information)

Additional investigations using confocal fluorescence microscopy and flow cytometry were then conducted. Polymer/cluster conjugates were labeled (Scheme S1) with two different amino-modified cyanine5.5 dyes, **Cy5.5** and **SulfoCy5.5**, following a previously described procedure.[13] **SulfoCy5.5** differs from **Cy5.5** by the presence of four sulfonate groups on the chromophore (Figure 1A), but both exhibit a similar fluorescence emission in the far-red/near-infrared ($\lambda_{em\ max}$≈700 nm). Two fluorescent polymer/cluster conjugates, **C4.2-Cy5.5** and **C4.8-SulfoCy5.5**, were synthesized as well as two reference copolymers without peptide-cluster **C0-Cy5.5** and **C0-SulfoCy5.5** for the *in cellulo* studies (Table 1, right).

To examine the specificity and the selectivity of the interaction with $\alpha_v\beta_3$-positive cells, the four fluorescent conjugates and the free peptide-cluster (labelled with **SulfoCy5.5**) were incubated with either HEKβ3 or HEKβ1 cells, over-expressing respectively $\alpha_v\beta_3$ and $\alpha_v\beta_1$ integrins. The results obtained by both confocal microscopy and flow cytometry experiments were in good agreement (Figures 2D, S8 and S9). In addition, no significant difference was noticed between the conjugates labelled with **Cy5.5** or

SulfoCy5.5 dyes. First, cell labeling was highly specific. HEKβ3 cells were very efficiently labeled by the polymer/cluster conjugates **C4.2-Cy5.5** and **C4.8-SulfoCy5.5** whereas no labeling was observed with the reference conjugates without peptide-cluster (**C0-Cy5.5** and **C0-SulfoCy5.5**). There were no non-specific interactions with the fluorescent polymers whatever the dye (with or without sulfonate negative charges). In addition, we observed that the cells tended to detach from the microscopy coverslips only in the presence of the polymer/cluster conjugates. Since cell-surface integrins are actively involved in adhesion mechanisms, this is an important proof that cRGD peptide/integrin interactions occurred and that for each conjugate the cRGD motifs are still functional. As seen by confocal microscopy, cell labeling was not restricted to the cell surface but rather distributed in the cytoplasm. This is of particular importance for targeted delivery applications. Compared to the free peptide-cluster, the labeling intensity of the HEKβ3 cells and thus the labeling sensitivity were significantly enhanced with the polymer/cluster conjugates. This can be ascribed to a combination of two different parameters, the higher brightness of the polymer conjugates that bear multiple dyes per chain compared to the free cluster (bearing only one dye) (see Supporting Information) and the higher binding efficiency to $\alpha_v\beta_3$-integrins of the polymer conjugates thanks to their polymultivalency.

Finally, comparison of the results with HEKβ3 and HEKβ1 cells indicated that the labeling was also selective. Labeling intensity was systematically higher for HEKβ3 cells (expressing more $\alpha_v\beta_3$-integrins) than for HEKβ1 cells. These results were consistent with those obtained with other cells lines expressing various levels of $\alpha_v\beta_3$-integrins, the M21 and M21L pair of melanoma cell lines and the integrin-positive U87MG glioblastoma cell line (Figure S9).

In conclusion, we have designed a new class of highly potent "polymultivalent" ligands that are very versatile. They could give rise in the future to various engineered systems such as random coils, single chain nanoparticles or larger assemblies. These biocompatible conjugates hold great promise for the vectorization of various kinds of diagnostic and/or therapeutic entities (attachment can be performed through a wide range of strategies) toward $\alpha_v\beta_3$-integrin-rich environments. For instance, the conjugates can be applied as biospecific fluorescent probes to study various biological processes involving $\alpha_v\beta_3$-integrins, both *in vitro* and *in vivo*. Futhermore, they may be used for the early diagnosis and the treatment of a large number of cancer tumors that overexpress $\alpha_v\beta_3$-integrins, especially because of their associated neoangiogenesis.

ASSOCIATED CONTENT

Supporting Information

Detailed experimental part, complementary NMR data, structural considerations about the polymer/peptide-cluster conjugates and their interaction with $\alpha_v\beta_3$-integrin-presenting targets, characterization of the fluorescent polymers as well as confocal microscopy and flow cytometry data with various cell lines. This material is available free of charge via the Internet at http://pubs.acs.org.

AUTHOR INFORMATION

Corresponding Author

* E-mails: arnaud.favier@univ-lyon1.fr; jean-luc.coll@univ-grenoble-alpes.fr; didier.boturyn@univ-grenoble-alpes.fr

ACKNOWLEDGMENT

We are grateful to Cristina Cepraga for the synthesis of Poly(NAM-*stat*-NAS) copolymer, the ICMG Chemistry Nanobio Platform, Grenoble, for support on peptide synthesis, Alexei Grichine, Jacques Mazzega and Mylene Pezet from the MicroCell imaging facility of IAB, Grenoble, for their technical help, the NMR Polymer Center of Institut de Chimie de Lyon (ICL, FR5223), Carlos Baleizao and José-Paulo Farinha (CQFM, Instituto Tecnico Superior, Lisbon, Portugal) for the absorption and fluorescence emission spectra. We also thank Région Rhône-Alpes (ARC1 Santé) and La Ligue contre le Cancer – Comité du Rhône for financial support. DD acknowledges a PhD grant from the French Ministry of Research and Education.

REFERENCES

(1) Mammen, M.; Choi, S.-K.; Whitesides, G. M., *Angew. Chem. Int. Ed.* **1998,** *37*, 2754.

(2) (a) Krishnamurthy, V. M.; Estroff, L. A.; Whitesides, G. M., Multivalency in Ligand Design. In *Fragment-based Approaches in Drug Discovery*, Wiley-VCH Verlag GmbH & Co. KGaA: 2006; pp 11. (b) Carlson, C. B.; Mowery, P.; Owen, R. M.; Dykhuizen, E. C.; Kiessling, L. L., *ACS Chem. Biol.* **2007**, *2*, 119. (c) Fasting, C.; Schalley, C. A.; Weber, M.; Seitz, O.; Hecht, S.; Koksch, B.; Dernedde, J.; Graf, C.; Knapp, E.-W.; Haag, R., *Angew. Chem. Int. Ed.* **2012,** *51*, 10472. (d) Cecioni, S.; Imberty, A.; Vidal, S., *Chem. Rev.* **2015,** *115*, 525. (e) Varner, C. T.; Rosen, T.; Martin, J. T.; Kane, R. S., *Biomacromolecules* **2015,** *16*, 43.

(3) Gestwicki, J. E.; Cairo, C. W.; Strong, L. E.; Oetjen, K. A.; Kiessling, L. L., *J. Am. Chem. Soc.* **2002,** *124*, 14922.

(4) (a) Martinez-Veracoechea, F. J.; Frenkel, D., *PNAS* **2011,** *108*, 10963. (b) Dubacheva, G. V.; Curk, T.; Mognetti, B. M.; Auzély-Velty, R.; Frenkel, D.; Richter, R. P., *J. Am. Chem. Soc.* **2014,** *136*, 1722.

(5) Poon, Z.; Chen, S.; Engler, A. C.; Lee, H.-i.; Atas, E.; von Maltzahn, G.; Bhatia, S. N.; Hammond, P. T., *Angew. Chem. Int. Ed.* **2010,** *49*, 7266.

(6) Martin, A. L.; Li, B.; Gillies, E. R., *J. Am. Chem. Soc.* **2009,** *131*, 734.

(7) Kumar, J.; Bousquet, A.; Stenzel, M. H., *Macromol. Rapid Commun.* **2011,** *32*, 1620.

(8) Ribeiro-Viana, R.; Sánchez-Navarro, M.; Luczkowiak, J.; Koeppe, J. R.; Delgado, R.; Rojo, J.; Davis, B. G., *Nat. Commun.* **2012,** *3*, 1303.

(9) Ringsdorf, H., *J. Polym. Sci.: Polym. Symp.* **1975,** *51*, 135.

(10) Pfaff, M.; Tangemann, K.; Müller, B.; Gurrath, M.; Müller, G.; Kessler, H.; Timpl, R.; Engel, J., *J. Biol. Chem.* **1994,** *269*, 20233.

(11) (a) Hynes, R. O., *Nat. Med.* **2002,** *8*, 918. (b) Kairbaan, H.-D., *Curr. Opin. Cell Biol.* **2008,** *20*, 514. (c) Keramidas, M.; Josserand, V.; Feige, J.-J.; Coll, J.-L., *Mol. Imaging Biol.* **2013,** *15*, 239.

(12) (a) Danhier, F.; Breton, A. L.; Préat, V., *Mol. Pharm.* **2012,** *9*, 2961. (b) Chen, X.; Plasencia, C.; Hou, Y.; Neamati, N., *J. Med. Chem.* **2005**, *48*, 1098. Mukhopadhyay, S.; Barnes, C.M.; Haskel, A.; Short, S.M.; Barnes, K.R.; Lippard, S.J., *Bioconj. Chem.* **2008**, *19*, 39. Li, Z.-B.; Cai, W.; Chen, K.; Wu, Z.; He, L.; Chen, X., *J. Nucl. Med.* **2007**, *48*, 1162. Jin, Z.H.; Josserand, V.; Foillard, S.; Boturyn, D.; Dumy, P.; Favrot, M.C.; Coll, J.L., *Mol. Cancer*, **2007**, *6*, 41.

(13) Cepraga, C.; Gallavardin, T.; Marotte, S.; Lanoe, P.-H.; Mulatier, J.-C.; Lerouge, F.; Parola, S.; Lindgren, M.; Baldeck, P. L.; Marvel, J.; Maury, O.; Monnereau, C.; Favier, A.; Andraud, C.; Leverrier, Y.; Charreyre, M.-T., *Polym. Chem.* **2013,** *4*, 61.

(14) Boturyn, D.; Coll, J.-L.; Garanger, E.; Favrot, M.-C.; Dumy, P., *J. Am. Chem. Soc.* **2004,** *126*, 5730.

(15) (a) Boturyn, D.; Defrancq, E.; Dolphin, G. T.; Garcia, J.; Labbe, P.; Renaudet, O.; Dumy, P., *J. Pept. Sci.* **2008,** *14*, 224. (b) Misra, S. K.; Kondaiah, P.; Bhattacharya, S.; Boturyn, D.; Dumy, P., *J. Mater. Chem. B* **2014,** *2*, 5758.

(16) (a) Garanger, E.; Boturyn, D.; Coll, J.-L.; Favrot, M.-C.; Dumy, P., *Org. Biomol. Chem.* **2006,** *4*, 1958. (b) Sancey, L.; Garanger, E.; Foillard, S.; Schoehn, G.; Hurbin, A.; Albiges-Rizo, C.; Boturyn, D.; Souchier, C.; Grichine, A.; Dumy, P.; Coll, J.-L., *Mol. Ther.* **2009,** *17*, 837**.** (c) Foillard, S.; Dumy, P.; D. Boturyn, D., *Org. Biomol. Chem.* **2009**, *7*, 4159. (d) Degardin, M.; Thakar, D.; Claron, M.; Richter, R. P.; Coche-Guérente, L.; Boturyn D., *J. Mater. Chem. B* **2017**, Advance article, DOI: 10.1039/C7TB00630F.

(17) (a) Chiefari, J.; Chong, Y. K.; Ercole, F.; Krstina, J.; Jeffery, J.; Le, T. P. T.; Mayadunne, R. T. A.; Meijs, G. F.; Moad, C. L.; Moad, G.; Rizzardo, E.; Thang, S. H., *Macromolecules* **1998,** *31*, 5559. (b) Favier, A.; Charreyre, M. T., *Macromol. Rapid Commun.* **2006,** *27*, 653.

(18) (a) Favier, A.; D'Agosto, F.; Charreyre, M. T.; Pichot, C., *Polymer* **2004,** *45* (23), 7821. (b) Favier, A.; Charreyre, M. T. Method for controlled free-radical polymerization. WO 04/055060, 2004.
(19) Bencini, M.; Ranucci, E.; Ferruti, P.; Manfredi, A.; Trotta, F.; Cavalli, R., *J. Polym. Sci. Part A: Polym. Chem.* **2008,** *46*, 1607.
(20) Galibert, M.; Sancey, L.; Renaudet, O.; Coll, J.-L.; Dumy, P.; Boturyn, D., *Org. Biomol. Chem.* **2010,** *8* (22), 5133.

For Table of Contents Only